2021 43rd Annual International Conference of the
IEEE Engineering in Medicine & Biology Society (EMBC)
Oct 31 - Nov 4, 2021. Virtual Conference

In silico study on radiobiological efficacy of Ac-225 and Lu-177 for PSMA-guided radiotherapy

Gabriele Birindelli[1], Milos Drobnjakovic[1], Volker Morath[2], Katja Steiger[3], Calogero D'Alessandria[2], Eleni Gourni[1], Ali Afshar-Oromieh[1], Wolfgang Weber[2], Axel Rominger[1], Matthias Eiber[2] and Kuangyu Shi[1]

***Abstract*— The good efficacy of radioligand therapy (RLT) targeting prostate specific-membrane antigen (PSMA) for the treatment of metastatic castration-resistant prostate cancer (mCRPC) has been recently demonstrated in several clinical studies. However, the treatment effect of ^{177}Lu-PSMA-ligands is still suboptimal for a significant fraction of patients. In contrast to external beam radiotherapy, the radiation dose distribution itself is strongly influenced by the heterogeneous tumour microenvironment. Although microdosimetry is critical for RLT treatment outcome, it is difficult to clinically or experimentally establish the quantitative relation. We propose an *in silico* approach to quantitatively investigate the microdosimetry and its influence on treatment outcome for PSMA-directed RLT of two different radioisotopes ^{177}Lu and ^{225}Ac. The ultimate goal is optimize the combined ^{177}Lu and ^{225}Ac-PSMA therapy and maximize the anti-tumour effect, while minimizing irradiation of off-target tissues.**

***Clinical relevance*— With the proposed hybrid model we show that ^{177}Lu-PSMA-ligands treatment assures a more homogeneously distributed dose and a lower dependency of the treatment outcome on the domain vascularisation. On the other hand, the ^{225}Ac-PSMA-ligands treatment shows a much stronger efficacy in killing tumor cells with an equivalent mean dose distribution even in an hypoxic environment.**

I. INTRODUCTION

The last decades have witnessed rapid acceleration in the impact of tumor-targeted radioligand therapy (RLT). Promising results have been obtained in the treatment of metastatic castration-resistant prostate cancer (mCRPC), known for its high burden of morbidity and mortality [1]. Prostate carcinoma is characterized by the increased expression of the specific type II transmembrane glycoprotein named prostate-specific membrane antigen (PSMA) [2]. Several studies have demonstrated the efficacy and safety of RLT for the treatment of mCRPC performed with Lutetium-177 (^{177}Lu-PSMA-ligands) [3], [4]. A recent meta-analysis shows biochemical and radiological responses in 46% and 37% of the patients, respectively [5]. Despite the early success, the relatively low linear energy transfer (LET) of the β-particle emitted by ^{177}Lu causes mostly single-strained DNA breaks leading to treatment resistance. A more potent alternative is represented by the α-emitter Actinium-225 (^{225}Ac-PSMA-ligands). The LET of the α-particle ($\sim$100 keV/μm), 500 times higher of the LET of the β-particle emitted by ^{177}Lu, induces with a higher probability a double-strand break of the DNA [6], [7]. A recent meta-analysis on ^{225}Ac-PSMA-ligands therapy indicates a remarkable efficacy of this targeted approach, with a response rates that exceed those published for ^{177}Lu-PSMA RLT [8]. However, the reduced range of α-particles in human tissues, i.e. ~ 50 μm for α-particles emitted by ^{225}Ac with respect to ~ 1.6 mm for β-particles emitted by ^{177}Lu, can strongly reduce the cross-fire effect in large tumors with poorly vascularized regions. Moreover, the injected activity of ^{225}Ac is limited by salivary gland toxicity. The complimentary advantages of α and β-emitting RLTs lead to the concept of "cocktail treatment" to maximize the antitumoral effect. It remains unclear how such a dual radionuclide treatment should be formulated and the potential treatment outcome. In the past decades, systems medicine has emerged as a tool to facilitate hypothesis generation, data integration, and patient-specific therapeutic development. Systems medicine has already been applied for the development of multi-modal imaging strategies [9]. Histology-driven computational simulation have been proposed to emulate real biological complexity of tissues [10], [11]. *In silico* modeling based on physiologically-based pharmaco-kinetic (PBPK) models can assist the optimization of PSMA-directed radioligand therapy. We propose an *in silico* approach aiming to optimise the treatment by combining different radionuclides such as ^{177}Lu and ^{225}Ac attached to PSMA ligands.

II. MATERIALS AND METHODS

In this section the mathematical model used to simulate the ^{225}Ac-PSMA-ligands and ^{177}Lu-PSMA-ligands spatiotemporal distributions, the PBPK model used to generate the arterial input function (AIF), the kernel method used to calculate the cumulated dose distributions and the employed materials are presented.

A. Stained tumor sections

Formalin fixed, paraffin embedded (FFPE) tissue sections were submitted to autoradiography and immunohistochemistry (IHC) for CD31 (vessel endothelium) was performed on a consecutive cut. The IHC was done with a primary rabbit anti-CD31 antibody (abcam ab28364, 1:50) processed and detected on a Bond RXm system (Leica) with a polymer detection kit (without post primary antibody).

B. Vessel map generation

The computational domain consists of extravascular space interspersed by vessels, which constitute holes in the mesh.

This work was funded by the Novartis FreeNovation program

[1]Department of Nuclear Medicine, Inselspital, University of Bern, 3010 Bern, Switzerland

[2]Department of Nuclear Medicine, Klinikum rechts der Isar, School of Medicine, Technical University of Munich, 81675 München, Germany

[3]Institute of Pathology, School of Medicine, Technical University of Munich, 81675 München, Germany

The tumor tissue, i.e. the extravascular space, is assumed to be homogeneously divided into two sub-compartments: the interstitial compartment where the labelled PSMA-ligands can move and bind to the cells surface and the cellular compartment. The parameters used to describe the interstitial and cellular fractional volumes are derived from literature [12]. The vessel map is generated contouring one tissue microsection stained with the CD31 antibody. Multiple regions of interest (ROIs) of 1.6×1.6 mm^2 with different degrees of vascularisation (1.0%, 2.3% and 3.2%) have been extracted from the stained microsection. The vascular fraction in the ROIs are comparable with other published values [13], [14]. The radio-pharmaceutical flux across the vessel walls is modelled by appropriate boundary conditions as described in Section II-C.

C. Multi-scale spatial-temporal models of PSMA-ligands dynamics

The radio-pharmaceutical enters the tumour interstitium from the vasculature. It is then transported through the interstitial volume by diffusion down concentration gradients and convection from regions of high to low interstitial fluid pressure (IFP). Finally, it exits via cellular uptake and backflow into the vasculature. The flux density of PSMA-ligands across vessel walls, J_v [nmol s^{-1} cm^{-2}], is assumed to be proportional to the difference between the concentrations on the vascular C_v [nmol ml^{-1}] and the interstitium C_i side:

$$J_\mathrm{v} = L_\mathrm{v}(C_\mathrm{v} - C_\mathrm{i}), \tag{1}$$

where L_v [cm s^{-1}] represents the vessel wall permeability. The spatio-temporal evolution of the interstitial PSMA-ligands concentration can be described by a convection-reaction-diffusion (CRD) equation as:

$$\partial_t C_\mathrm{i} = \nabla \cdot (D_\mathrm{PSMA} \nabla C_\mathrm{i}) - \nabla \cdot (\vec{v}\, R_f C_\mathrm{i}) - k_\mathrm{on} C_\mathrm{i}(R_0 - C_\mathrm{b}) + k_\mathrm{off} C_\mathrm{b} - \lambda_\mathrm{dec} C_\mathrm{i}, \tag{2}$$

where D_PSMA [cm^2 s^{-1}] is the diffusivity of PSMA-ligands, R_f is the movement coefficient between the molecule and its carrier, the terms $\nabla \cdot (D_\mathrm{PSMA} \nabla C_\mathrm{i})$ and $\nabla \cdot (\vec{v}\, R_f C_\mathrm{i})$ describe changes in interstitial radio-pharmaceutical concentration due to diffusion and convection, k_on [cm^3 nmol^{-1} s^{-1}] and k_off [s^{-1}] are respectively the association and dissociation rates, C_b is the bounded radio-pharmaceutical concentration [nmol ml^{-1}], R_0 [nmol ml^{-1}] is the PSMA binding sites density and λ_dec [s^{-1}] is the radionuclide decay constant.

The labelled molecule has a high-binding affinity for PSMA expressed on the prostate cancer cell surface. Moreover, PSMA undergoes an internalisation process that allows the radionuclide to be concentrated within the cell [15]. Demanding mass conservation and assuming first-order kinetics, the rates of change of bounded and internalized PSMA-ligands concentrations, C_int, can be written as

$$\partial_t C_\mathrm{b} = k_\mathrm{on} C_\mathrm{i}(R_0 - C_\mathrm{b}) - k_\mathrm{off} C_\mathrm{b} - k_\mathrm{int} C_\mathrm{b} - \lambda_\mathrm{dec} C_\mathrm{b}, \tag{3}$$

and

$$\partial_t C_\mathrm{int} = k_\mathrm{int} C_\mathrm{b} FV_\mathrm{i}/FV_\mathrm{c} - k_\mathrm{rel} C_\mathrm{int} - \lambda_\mathrm{dec} C_\mathrm{int}, \tag{4}$$

where k_int [s^{-1}] and k_rel [s^{-1}] are the internalization and the release rates respectively and FV_i and FV_c are the fractional volumes of tumour interstitium and cells within a voxel respectively. The radio-pharmaceutical flux across the vessel walls is modelled via Neumann boundary conditions imposed on the vessel boundaries as

$$\vec{\mathrm{n}} \cdot (D_\mathrm{PSMA} \nabla C_\mathrm{i}) = J_\mathrm{v}, \tag{5}$$

where $\vec{\mathrm{n}}$ is the normal unit vector to the respective boundary segment. No-flux boundary conditions were applied to the edges of the vessel map. Table I lists the tissue physiological parameter estimates deduced from the literature [12], [16], [17].

TABLE I

MODEL PARAMETER VALUES USED IN SIMULATIONS

Parameter	Value	Ref.
Vessel wall permeability	3.3×10^{-4} cm s^{-1}	[17]
Diffusivity	8.7×10^{-7} cm^2 s^{-1}	[16]
Receptor density	4.089×10^{-2} nmol ml^{-1}	fitted
Association rate	7.7×10^{-1} ml nmol^{-1} s^{-1}	[12]
Dissociation rate	7.7×10^{-4} s^{-1}	[12]
Internalization rate	1.67×10^{-5} s^{-1}	[12]
Release rate	2.67×10^{-6} s^{-1}	[12]
Fractional interstitial volume	39%	[12]
Fractional cellular volume	61%	[12]
^{177}Lu decay constant	1.197×10^{-6} s^{-1}	
^{225}Ac decay constant	8.087×10^{-7} s^{-1}	

D. Tissue oxygenation simulation

To study the effect of the presence of hypoxic tissue on the treatment outcome, we modelled the tissue oxygenation. Accordingly to the published literature, the oxygen transport is modelled as a purely diffusive process that is in equilibrium with cellular oxygen consumption [10], [11]. The cellular oxygen consumption has been modelled considering Michaelis–Menten kinetics [18]. The paramenters used in the oxygenation reaction-diffusion model have been derived by literature [10], [11].

E. Physiologically based pharmacokinetic model

Physiologically based pharmacokinetic (PBPK) models are compartment-based models used to simulate the absorption, distribution, metabolism, and excretion of the injected compound in the human body [19]. An existing and validated PBPK model [12] for RLT studies has been adopted to calculate the arterial input function (AIF), i.e. the time dependant vascular concentration of PSMA-ligands C_v, used in our CRD model. The PBPK model for PSMA-ligands was adapted to be compatible with mouse physiology. Mouse physiological variables were either based on rescaling human parameters or derived from literature [20], [21], [22], [23], [24]. The tumor tissue was treated as a xenograft, therefore parameters such as vascular and interstitial fraction, receptor density, PSMA-ligands binding constants, degradation and internalization rates were assumed to be the same as in humans [12]. The injected amount of radio-pharmaceutical was chosen to obtain a mean deposited dose in the prostate tumor model of 10 Gy after 20 days post-injection.

F. Absorbed dose and cell survival probability

The absorbed dose in each voxel of the domain has been calculated accordingly to the MIRD formalism [25]. The mean absorbed dose $D(r_T, T_D)$ [Gy] to target voxel r_T over a defined period T_D is defined as

$$D(r_T, T_D) = \sum_{r_s} \tilde{A}(r_S, T_D) S(r_T \leftarrow r_S), \qquad (6)$$

where $\tilde{A}(r_S, T_D)$ [Bq] is the time-integrated activity in source voxel r_S over the period T_D and $S(r_T \leftarrow r_S)$ is the radionuclide-specific quantity representing the mean absorbed dose to the target voxel r_T per unit activity present in the source voxel r_S. In this work the S values for each radionuclide are calculated with the use of MIRD-cell (V2.0) [26]. The probability that a cell survives is calculated accordingly to the linear quadratic model

$$P_S = e^{-\alpha D - \beta D^2}, \qquad (6)$$

where α and β are the linear quadratic parameters that characterize the cellular response to the ionizing radiation and D [Gy] is the absorbed dose [27]. The cell survival curve for α-particle radiation is log-linear at low as well as high absorbed doses. The survival probability equation can be consequently simplified as

$$P_S = e^{-D/D_0}, \qquad (7)$$

where D_0 is the absorbed dose required to yield a survival fraction of 37% [28]. The parameters used to calculate the cells survival probability are resumed in Table II.

TABLE II
PARAMETERS USED FOR THE CELLS SURVIVAL PROBABILITY CALCULATIONS

Parameter	Normoxic	Hypoxic	Ref.
α	0.15 Gy^{-1}	0.107 Gy^{-1}	[29]
β	0.048 Gy^{-2}	0.024 Gy^{-2}	[29]
D_0	0.7 Gy	1.18 Gy	[30]

III. RESULTS AND DISCUSSION

In the following sections the simulation results are presented and discussed. At first, the dose distribution simulations are analysed for both the considered radionuclides. Then, the results on the distribution of cell survival probability in hypoxic tumor microenvironment are discussed.

A. Dose distribution in tumor microenvironment

With the use of the CRD model we simulate the radionuclide distribution into the tumor microenvironment. Once the activity distribution is recovered, for each radionuclide the kernel-based method is used to calculate the dose distribution in the domain. In Figure 1 the dose distributions for each radionuclide at ten days post injection are shown. The larger range covered by the β-particles emitted by ^{177}Lu produces a more homogeneous dose distribution in the tumor microenvironment. The higher "cross-fire" effect induced by the β-particles has an impact on the standard deviation of the deposited dose in the domain. Indeed, the statistical analysis performed in all the ROIs shows in all cases a higher standard deviation in the dose distributions obtained with ^{225}Ac. The percentage dose difference map shows a stronger dose deposition in the vessels neighbourhood for ^{225}Ac-PSMA compared to ^{177}Lu-PSMA. The higher dose deposition given by ^{225}Ac near vessels results in a globally higher mean deposited dose in the highly vascularized domain as shown in the statistical analysis.

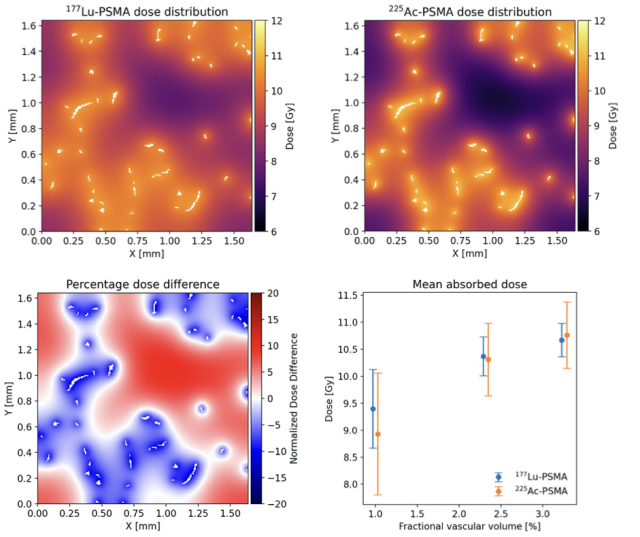

Fig. 1. Top: dose distributions obtained in the ROI with lowest vascularization ten days post-injection with ^{177}Lu-PSMA (left) and ^{225}Ac-PSMA (right). Bottom left: percentage dose difference between the dose distributions obtained with ^{177}Lu and ^{225}Ac. Bottom right: statistical analysis of the mean dose distributions calculated in all the ROIs, the vertical lines represent the standard deviation.

B. Radiobiological efficacy analysis

Applying the linear-quadratic modelling to the dose maps, the cell survival probability for both ^{225}Ac-PSMA-ligands or ^{177}Lu-PSMA-ligands has been calculated. Figure 2 depicts the cell survival probability distribution for the examined radionuclides. For the same mean irradiation dose at ten days post-injection, the ^{225}Ac-PSMA-ligand has a significantly higher cell-killing potency. This finding is consistent with the reported higher probability of double-stranded break induction by the α particles, which are more difficult for the cell to repair. Although the ^{177}Lu-PSMA-ligand is overall less lethal, the longer range of β-particles enables the ^{177}Lu based treatment to be less dependent on the degree of domain vascularization, as can be seen by the smaller standard deviation in the mean cell survival probability for all the examined ROIs.

IV. CONCLUSIONS

The proposed hybrid model can give a deep insight into the efficacy of ^{177}Lu-PSMA-ligands and ^{225}Ac-PSMA-ligands at the tumor microenvironment level. The ^{177}Lu-PSMA-ligands treatment assures a more homogeneously distributed

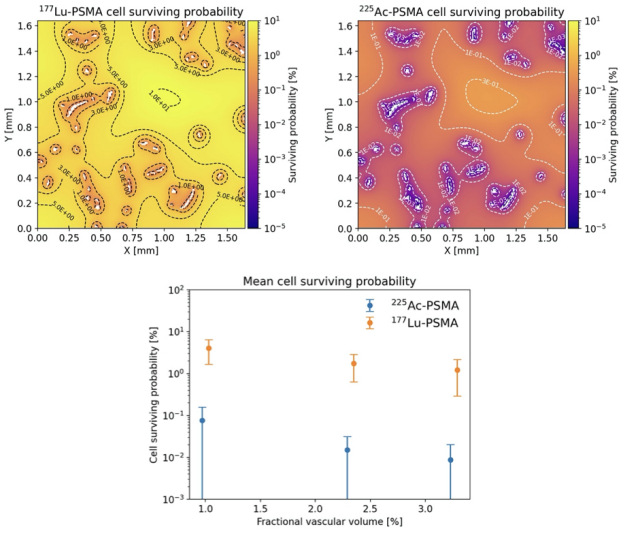

Fig. 2. Top: Distribution of cell survival probabilities in the ROI with the lowest vascularization ten days post-injection with ^{177}Lu-PSMA (left) and ^{225}Ac-PSMA (right). Bottom: statistical analysis of the mean cell survival probability calculated for each of the examined ROIs, the vertical lines represent the standard deviation.

dose and a lower dependency of the treatment outcome on the domain vascularisation. On the other hand, the ^{225}Ac-PSMA-ligand treatment shows a much stronger efficacy in killing tumor cells with an equivalent mean dose distribution. Further optimisation and validation of this model on experimental data is ongoing.

REFERENCES

[1] HELGSTRAND, John T., et al. Trends in incidence and 5-year mortality in men with newly diagnosed, metastatic prostate cancer—A population-based analysis of 2 national cohorts. Cancer, 2018, 124.14: 2931-2938.

[2] SWEAT, Susan D., et al. Prostate-specific membrane antigen expression is greatest in prostate adenocarcinoma and lymph node metastases. Urology, 1998, 52.4: 637-640.

[3] KRATOCHWIL, Clemens, et al. PSMA-targeted radionuclide therapy of metastatic castration-resistant prostate cancer with 177Lu-labeled PSMA-617. Journal of Nuclear Medicine, 2016, 57.8: 1170-1176.

[4] HOFMAN, Michael S., et al. [177Lu]-PSMA-617 radionuclide treatment in patients with metastatic castration-resistant prostate cancer (LuPSMA trial): a single-centre, single-arm, phase 2 study. The Lancet Oncology, 2018, 19.6: 825-833.

[5] YADAV, Madhav Prasad, et al. Radioligand therapy with 177Lu-PSMA for metastatic castration-resistant prostate cancer: a systematic review and meta-analysis. American Journal of Roentgenology, 2019, 213.2: 275-285.

[6] TAFRESHI, Narges K., et al. Development of targeted alpha particle therapy for solid tumors. Molecules, 2019, 24.23: 4314.

[7] KRATOCHWIL, Clemens, et al. Patients Resistant Against PSMA-Targeting α-Radiation Therapy Often Harbor Mutations in DNA Damage-Repair–Associated Genes. Journal of Nuclear Medicine, 2020, 61.5: 683-688.

[8] SATAPATHY, Swayamjeet, et al. Evolving role of 225 Ac-PSMA radioligand therapy in metastatic castration-resistant prostate cancer—a systematic review and meta-analysis. Prostate Cancer and Prostatic Diseases, 2021, 1-11.

[9] WANG, Qian, et al. Exploring the quantitative relationship between metabolism and enzymatic phenotype by physiological modeling of glucose metabolism and lactate oxidation in solid tumors. Physics in Medicine & Biology, 2015, 60.6: 2547.

[10] MÖNNICH, David, et al. Modelling and simulation of [18F] fluoromisonidazole dynamics based on histology-derived microvessel maps. Physics in Medicine & Biology, 2011, 56.7: 2045.

[11] SHI, Kuangyu, et al. Matching the reaction-diffusion simulation to dynamic [18F] FMISO PET measurements in tumors: extension to a flow-limited oxygen-dependent model. Physiological measurement, 2017, 38.2: 188.

[12] BEGUM, Nusrat J., et al. The effect of ligand amount, affinity and internalization on PSMA-targeted imaging and therapy: A simulation study using a PBPK model. Scientific reports, 2019, 9.1: 1-8.

[13] ŁUCZYŃSKA, Elżbieta, et al. Correlation between CT perfusion and clinico-pathological features in prostate cancer: a prospective study. Medical science monitor: international medical journal of experimental and clinical research, 2015, 21: 153.

[14] JAIN, Rakesh K. Determinants of tumor blood flow: a review. Cancer research, 1988, 48.10: 2641-2658.

[15] LIU, He, et al. Constitutive and antibody-induced internalization of prostate-specific membrane antigen. Cancer research, 1998, 58.18: 4055-4060.

[16] SWABB, Edward A.; WEI, James; GULLINO, Pietro M. Diffusion and convection in normal and neoplastic tissues. Cancer research, 1974, 34.10: 2814-2822.

[17] JAIN, Rakesh K. Transport of molecules across tumor vasculature. Cancer and Metastasis Reviews, 1987, 6.4: 559-593.

[18] DAŞU, Alexandru; TOMA-DAŞU, Iuliana; KARLSSON, Mikael. Theoretical simulation of tumour oxygenation and results from acute and chronic hypoxia. Physics in Medicine & Biology, 2003, 48.17: 2829.

[19] ZHUANG, Xiaomei; LU, Chuang. PBPK modeling and simulation in drug research and development. Acta Pharmaceutica Sinica B, 2016, 6.5: 430-440.

[20] LYONS, Michael A., et al. A physiologically based pharmacokinetic model of rifampin in mice. Antimicrobial agents and chemotherapy, 2013, 57.4: 1763-1771.

[21] BI, Youwei, et al. A whole-body physiologically based pharmacokinetic model of gefitinib in mice and scale-up to humans. The AAPS journal, 2016, 18.1: 228-238.

[22] SINGH, Shalini, et al. Quantitative volumetric imaging of normal, neoplastic and hyperplastic mouse prostate using ultrasound. BMC urology, 2015, 15.1: 1-11.

[23] AGGARWAL, Saurabh, et al. Comparative study of PSMA expression in the prostate of mouse, dog, monkey, and human. The prostate, 2006, 66.9: 903-910.

[24] ROY, Jyoti, et al. Identifying an appropriate animal model to examine preservation of salivary function with PSMA targeted radiotherapies. Journal of Nuclear Medicine, 2018, 59.supplement 1: 1255-1255.

[25] BOLCH,Wesley E., et al.MIRD Pamphlet No. 17: The Dosimetry of Nonuniform Activity Distributions—Radionuclide S Values at the Voxel Level. Journal of Nuclear Medicine, 1999, 40.1: 11S-36S

[26] VAZIRI, Behrooz, et al. MIRD pamphlet no. 25: MIRDcell V2. 0 software tool for dosimetric analysis of biologic response of multicellular populations. Journal of Nuclear Medicine, 2014, 55.9: 1557-1564.

[27] MCMAHON, Stephen Joseph. The linear quadratic model: usage, interpretation and challenges. Physics in Medicine and Biology, 2018, 64.1: 01TR01.

[28] SGOUROS, George, et al. MIRD Pamphlet No. 22 (abridged): radiobiology and dosimetry of α-particle emitters for targeted radionuclide therapy. Journal of nuclear medicine, 2010, 51.2: 311-328.

[29] WANG, J. Z.; LI, X. A.; MAYR, N. A. Dose escalation to combat hypoxia in prostate cancer: a radiobiological study on clinical data. The British journal of radiology, 2006, 79.947: 905-911.

[30] BARENDSEN, G. W., et al. The effect of oxygen on impairment of the proliferative capacity of human cells in culture by ionizing radiations of different LET. International Journal of Radiation Biology and Related Studies in Physics, Chemistry and Medicine, 1966, 10.4: 317-327.